International Journal of Automotive Technology, Vol. 6, No. 4, pp. 305–314 (2005)

1229-9138/2005/022-01

COMMON RAIL INJECTOR MODIFIED TO ACHIEVE A MODULATION OF THE INJECTION RATE

A. FICARELLA[1], A. GIUFFRIDA[2]* and R. LANZAFAME[2]

[1]University of Lecce, Department of Engineering for Innovation, Via per Arnesano, 73100 Lecce, Italy
[2]University of Catania, Department of Industrial and Mechanical Engineering, Viale Andrea Doria 6, 95125 Catania, Italy

(Received 11 September 2004; Revised 14 January 2005)

ABSTRACT–Injection rate shape control is one feature of a diesel fuel injection system that is strongly desired at this time. In the conventional common rail system, it is difficult to control the injection rate since the fuel pressure is constant during the injection period, resulting in a nearly rectangular rate shape. In order to look into possible injection modulations, injectors equipped with standard and geometrically modified control valves were investigated in detail by means of computer modelling and simulation. Experiments were carried out to validate the feasibility of such a shaping. The results of this study show a noteworthy dependence of the fuel rate on geometrical modifications in the piloting stage of the injector.

KEY WORDS : Common rail, Injection rate, Hydro grinding, Modulation, Initial injection quantity

1. INTRODUCTION

The compression ignition engine, or diesel engine, with its bigger compression ratios if compared to the spark-ignition (SI) engine, offers a higher thermodynamic efficiency. Additionally, the diesel engine with its less pumping losses due to the throttled intake charge as in an SI engine and with the increased thermal efficiency, offers increased fuel economy when compared to an SI engine. Nowadays, the direct injection (DI) diesel engine is the most efficient engine available for road vehicles. Thus, its use should be largely promoted. However, diesel engines emit more NOx and PM than other competing engines. Hence, the challenge in diesel engine development consists of reducing NOx and PM while maintaining their superiority with respect to fuel consumption. Traditionally there has been a contrasting relationship between PM and NOx. Due to very stringent legislation for PM in the future, particle traps are probably going to be used.

Efforts to reduce NOx have increased PM and vice versa. But traps change this situation and better possibilities emerge for treating NOx emissions with engine related means, such as injection timing, EGR and fuel rate shaping.

This work is focused on the possibility of shaping the fuel rate, especially at the early period of injection.

Among the studies dealing with injection modulation, the researches developed by AVL (Herzog, 1989; Erlach *et al.*, 1995) are probably the most outstanding. They concluded that the fuel rate at the beginning of the injection period should be rather low to minimize the heat released during the premixed combustion and to avoid too rapid combustion, then pressure and temperature rise and NOx formation. There is also experimental evidence that too high fuel rate at the injection beginning gives higher NOx emissions. Thus, a considerable reduction of NOx is achieved when the initial flow rate is decreased from the very high level typical for high pressure injection systems.

Considering the electronically controlled common rail (CR) injector (Stumpp and Ricco, 1996), the injection profile depends on both the fluid dynamics of the flow inside the injector and the dynamic response of the system itself. Thus, due to the constant fuel pressure in the rail, it is very difficult to modulate the injection rate according to the engine operating conditions. However, without modifying the injection system (pump, rail, regulators), variations in the flow characteristics of the control valve, the piloting stage of the injector, may be realized in order to achieve, as a significant result, the modification of the injection rate especially in the early stage of injection (Carlucci *et al.*, 2003).

The electro injector for CR systems (Figure 1), until

*Corresponding author. e-mail: agiuffri@diim.unict.it

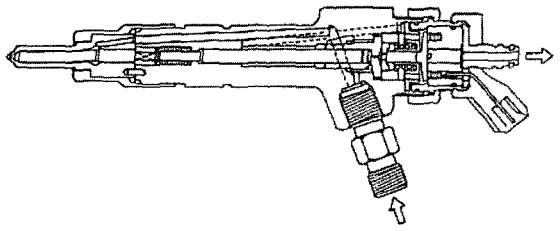

Figure 1. CR injector (Stumpp and Ricco, 1996).

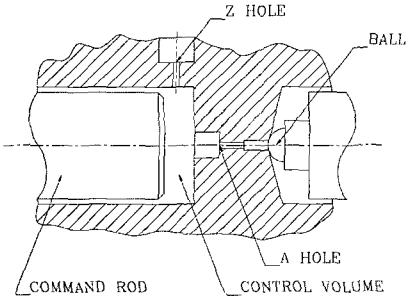

Figure 2. Details of the piloting stage of the injector.

the solenoid valve is not excited, does not allow injection. With reference to Figure 2, when the current signal excites the solenoid, fuel moves from the control volume through the A hole, whereas other fuel enters the control volume from the Z hole. These fuel flows modulate the pressure level inside the control volume, causing the command rod to stretch, then to move together with the needle which leaves its seat, so that injection occurs.

In order to shape the fuel rate, such a pressure control should be oriented to a less accentuated decrease as long as current excites the solenoid. This event is expected to drive the needle with a slower velocity during its upward movement. However, if pressure inside the control volume increases more quickly when the solenoid is no more energized and there is no flow through the A hole, the needle will be driven with a faster velocity during its downward movement. Thus, a modulation at the beginning of the injection and a sharp cutoff at its end should occur. The problem of a reduction of the fuel rate in the first stage of injection has been mentioned, but a sharp end of injection should allow to minimize hydrocarbon and soot emissions resulting from fuel entering the cylinder late in the cycle with poor spray development (Nehmer and Reitz, 1994). Figure 3 shows a qualitative comparison between the standard injection rate and the modified one according to the previous considerations.

Considering the functioning principle of the injector, there are several possibilities to achieve an injection shaping with a smoother and a steeper injection rate in

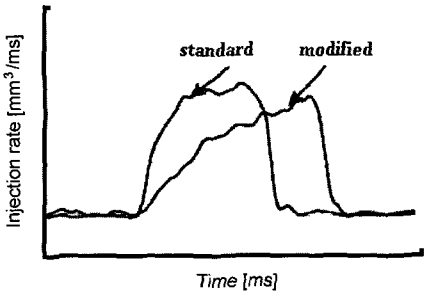

Figure 3. Qualitative comparison between standard and modified injection rates.

the initial and final stage respectively. A proper combination of geometrical and mechanical parameters of the control valve elements may be realized as in De Risi *et al.* (2002). However, modifying the discharge properties of the Z and A holes is a very easy intervention. In order to achieve the above mentioned modulation of the control volume pressure, the discharge properties of the Z and A holes are to be increased and reduced respectively. However, in the current work, starting from a standard commercial valve, a decrease in the discharge properties of the A hole is to be excluded. The possibility of an enlargement of the Z hole was already investigated by Amoia *et al.* (1997), where a theoretical sensitivity analysis showed an enlargement of the Z hole causes, among other effects:

(1) the increase of the time necessary to rise up to the maximum needle lift,
(2) the reduction of the time necessary to close the nozzle flow area,
(3) the consequent reduction of the injection duration.

It is well known that the development of a suitable numerical model for the injection system behaviour is very useful to predict the effects of the design parameters on fuel injection. There is a great deal of technical works dealing with the optimisation of the diesel injection systems and reflecting the importance of this task in engine improvement and design. As highlighted by several studies (Digesù *et al.*, 1994; Amoia *et al.*, 1997; Desantes *et al.*, 1999), a theoretical model of the injector dynamic behaviour is the first step to improve the control over the spray combustion process in diesel engines, in order to achieve lower fuel consumption and exhaust emissions.

Here, the injection behaviour of a Bosch CR injector of the first generation, equipped with different control valves, is investigated by theoretical and experimental points of view. In the next sections brief descriptions of the model and the experimental activity will follow, then results and significant trends due to the control valve modifications will be presented.

2. INJECTION SIMULATION

In order to study the performance of the injector, a specific model was developed. Governing equations were solved in the AMESim® environment (Imagine, 2002), where proper equations where added and implemented by the authors in order to tune the overall model.

Once the injector geometry and the physical properties of the fuel have been fixed, the model inputs consist of the rail pressure, the delivery (engine chamber) pressure, and the solenoid current. As a matter of fact, the injector is similar to a variable orifice with two fixed pressure levels across it, whereas its opening degree is commanded by the exciting current. The main outputs are pressure evolutions in all the injector chambers, volumetric and mass flow rates and the behaviour of the injector movable elements. Rail pressure and delivery (engine chamber) pressure were assumed to be constant.

2.1. Electromagnetic Model

The model realized to simulate the fluid dynamic bahaviour of the injector lacks of a detailed lay-out of the magnetic circuit. However, since the main result of this circuit is the force causing the movement of the masses inside the piloting stage, this force is modelled as a function depending on both exciting current and anchor position. It was obtained by fitting experimental data (Ficarella *et al.*, 1999).

2.2. Mechanical Model

All the injector components are modelled like a mass-spring-damper assembly, i.e. like a simple forced harmonic oscillator, according to the Newton's law. All the forces acting on the mass are taken into account: electromagnetic force, spring preloads, pressure forces and mass to mass interactions (impact forces). Every single element of the injector is schematised according to one or more masses, depending on its dimensions. Considering the command rod-needle assembly, it is subject to an axial deformation which is not negligible if compared to needle lift, so that maximum assembly lift depends on rail pressure (Henein *et al.*, 2002). Owing to the axial load (F_N), the deformed length l of the elements is evaluated as

$$l = l_0 \cdot \left(1 - \frac{F_N}{E \cdot S}\right) \tag{1}$$

being l_0 the un-deformed length, S its cross section and E the modulus of elasticity of the material.

As it was previously mentioned, possible impacts may occur between the movable parts, especially with reference to the masses inside the control valve. These forces are modelled according to the suggestions provided by Lee *et al.* (2002).

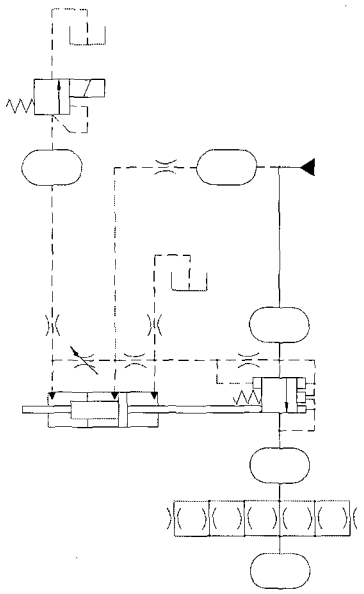

Figure 4. Injector equivalent hydraulic circuit.

2.3. Hydraulic Model

The equivalent hydraulic circuit of the injector is shown in Figure 4. Continuous lines are used to represent the main connecting ducts, whereas dashed lines represent pilot and vent connections. The hydraulic parts of the injector are modelled as variable or fixed orifices and uniform pressure chambers on the basis of a zero dimensional modelling approach. Instead, the pipes connecting the rail to the injector inlet and the injector inlet to the injection chamber are modelled according to a one dimensional modelling approach.

2.3.1. Orifices discharge properties

Modelling the hydraulic discharge properties of the various orifices inside the injector is fundamental for a correct simulation of its fluid dynamic behaviour. Here it is noteworthy to point out that the flow rate through the Z hole was modelled as

$$Q_{Zhole} = c_Z \cdot \sqrt{p_{in} - p_{cv}} \tag{2}$$

where c_Z relates the volumetric flow rate through the hole to a fixed pressure drop. It depends on the mean pressure between the inlet (p_{in}) and the control volume pressure (p_{cv}), so that it takes density variability into account. This hole is characterized by relatively small pressure drops, so that cavitation should not occur (Ficarella *et al.*, 1999) and the previous formulation is strictly sufficient.

On the other side, flow cavitation cannot be neglected in the outlet orifices from the control volume. The A hole

and the truncated cone lateral surface due to the ball movement (Figure 2) represent the series of two orifices for the fuel leaving the control volume. However, when the ball exceeds almost one half of its maximum lift, the minimum flow area moves from the ball seat towards the A hole. Now, the latter governs the fuel discharge. Owing to the considerably large pressure drop across the A hole, it prevalently works under cavitating conditions and its discharge properties are to be accurately modelled. Flow rate through the A hole was calculated according to the standard equation

$$Q_{Ahole} = C_{d,Ahole} \cdot n_h \cdot \left(\frac{\pi}{4} \cdot d_{Ahole}^2\right) \cdot \sqrt{\frac{2}{\rho} \cdot (p_{cv} - p_d)} \qquad (3)$$

and the formulations reported by Nurick (1976) and Schmidt and Corradini (1997) were adopted to model the discharge coefficient under cavitating conditions as

$$C_{dcav} = C_c \cdot \sqrt{\frac{p_{cv} - p_v}{p_{cv} - p_d}} = C_c \cdot \sqrt{1 + \frac{1}{CN}} \qquad (4)$$

CN is the cavitation number, whose increase determines larger flow cavitation and p_v and p_d are the vapour and delivery pressures, respectively. The contraction coefficient (C_c) is a parameter strongly dependent on the hole geometry. It was fixed according to experimental flow measures at a feeding pressure equal to 10 MPa on a hydraulic test bench, with a back pressure equal to the atmospheric one.

The injector studied in this work was equipped with a VCO nozzle. Its discharge properties were modelled according to Klomp (1999). Inside the nozzle the fuel flow may be divided into three paths: the first is the annular conical accelerating flow between needle and injector body, the second is where the flow is turned when it enters the hole and the third consists of the hole itself. Nevertheless, the final formulation is only one:

$$Q_{inj} = C_d^* \cdot n_h \cdot \left(\frac{\pi}{4} \cdot d_h^2\right) \cdot \sqrt{\frac{2}{\rho} \cdot (p_{inj} - p_{cyl})} \qquad (5)$$

where n_h is the number of nozzle holes, d_h is the hole diameter and

$$C_d^* = \frac{C_{d0}}{\sqrt{\left(\frac{C_{d0}}{Z} \cdot \frac{d_h}{x_n}\right)^2 + 1}} \qquad (6)$$

represents the overall discharge coefficient. As regards Equation (6), Z is a dimensionless parameter taking nozzle geometry into account, x_n represents the needle lift and C_{d0} is the discharge coefficient of one of the holes finishing up in the combustion chamber. The value for

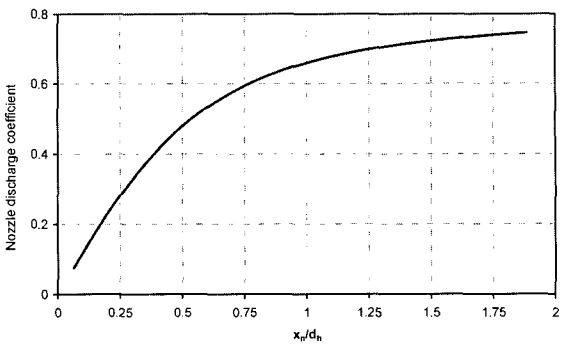

Figure 5. Nozzle discharge coefficient.

this discharge coefficient should be fixed according to the discharge properties declared for the nozzle itself. In Klomp (1999) a wide range of C_{d0} values is examined from 0.63 up to 0.8, considering that hydro grinding process considerably increases nozzle discharge properties. Here, a proper C_{d0} was chosen in order to achieve the declared flow rate (13.33 ± 0.27 mm^3/ms) with a feeding pressure equal to 10 MPa and the needle lift fixed equal to 250 μm (Kampmann *et al.*, 1996). Figure 5 shows the overall discharge coefficient as reported in Eq. (6).

2.3.2. Lumped volumes and pipes

Pressure level (p_{inj}) inside the injection volume (Figure 6) is to be evaluated as accurate as possible since it governs the injection rate according to Eq. (5). Such a pressure is evaluated on the basis of the continuity equation

$$\frac{dp_{inj}}{dt} = \frac{\beta}{V_{inj}} \cdot \left(\Sigma_k Q_k - \frac{dV_{inj}}{dt}\right) \qquad (7)$$

The sum of all the volumetric flow rates in the previous equation takes into account

(1) the feeding fuel rate from the pipe connecting the injector inlet to the injection volume,
(2) the injection rate,
(3) the leakage fuel rate,

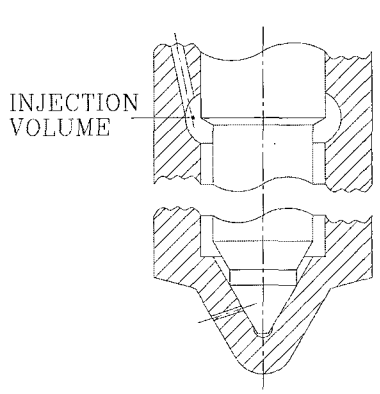

Figure 6. Injection volume just upstream the needle seat.

(4) and the entrained flow due to the fuel adhering to the needle, which is simultaneous to the needle movement. This flow path is represented by the annulus from the inner wall of the nozzle holder to the needle external circumference.

It is to be pointed out that in modelling the nozzle, the dimension of the above mentioned annulus was supposed to be unable to introduce a relevant flow resistance. As a matter of fact, this gap is wider enough if compared to the clearance between parts having relative motions to each other. The pumping effect of the needle is accounted for in the volume variation term.

Waves propagation phenomena in pipes connecting two chambers are considered according to the following equation

$$\frac{\partial p}{\partial t} = -\frac{\beta}{A} \cdot \frac{\partial Q}{\partial x} \tag{8}$$

where A is the inner cross-sectional area of the pipe and β is the fuel bulk modulus. The compressibility of the fluid and the expansion of the pipe wall with pressure are taken into account by using an effective bulk modulus (Imagine, 2002). Pipe friction is accounted for by using a factor depending on the Reynolds number and the relative roughness. As regards the inertia of the fluid, a flow rate state variable at one end of the pipe is considered. There is also a state variable representing the pressure at the other end:

$$\frac{\partial Q}{\partial t} = \frac{A}{\rho} \cdot \frac{\partial p}{\partial x} - v \cdot \frac{\partial Q}{\partial x} - \frac{\lambda \cdot Q^3}{2 \cdot D \cdot A \cdot |Q|} \tag{9}$$

where D is the pipe diameter, v is the mean flow velocity and λ is the friction factor.

2.3.3. Fluid model

The fuel properties consisting of density, bulk modulus and dynamic viscosity are evaluated during the simulation. A particular submodel (Imagine, 2000) forces the use of properties of the fuel based on measurements in the temperature range from 10 to 120°C and the pressure range from 0 to 200 MPa. Outside these ranges the fluid properties are obtained by extrapolation. The bulk modulus used for the fuel is an adiabatic one and hence is suitable for fast acting systems such as the one considered in this work.

3. EXPERIMENTAL EQUIPMENT AND PROCEDURE

Experimental tests were carried out at the laboratories of Bosch-CSIT (Bari, Italy).

The acquired data consisted of the exciting current, the fuel injection rate and the needle lift, each one with the same sampling frequency fixed to 33 kHz. The excitation time (ET) was varied during the experiments with variable steps, so a wide range of operating points was investigated. The experimental campaign allowed to validate the model and to make it reliable for the next study regarding the sensitivity of the injector behaviour with respect to variations in the Z hole discharge properties.

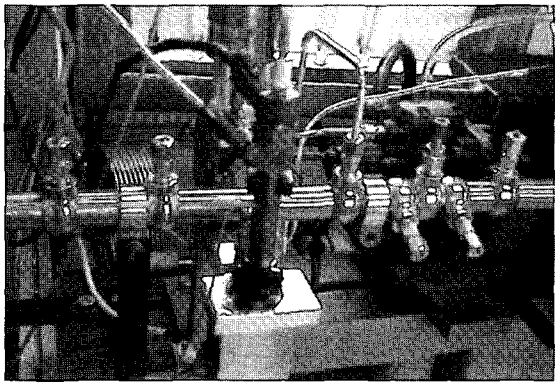

Figure 7. Experimental hydraulic test bench.

3.1. Injection Rate

The injected fuel rates were measured according to the method suggested by Bosch (1966). Figure 7 shows the injector fed by a pipe from the rail. It is put inside a proper adaptor, where there is the pressure transducer, located downstream the nozzle holes. The measuring tube is opportunely rolled up.

It was demonstrated (Bosch, 1966) that such a measuring device is an absolute instrumentation, since the relationship between the over pressure (Δp_{tube}), generated during injection and acquired by the transducer, and the instantaneous fuel rate (Q_{inj}) may be theoretically evaluated. The relationship representing this link is

$$Q_{inj} = \frac{A \cdot a}{\beta} \cdot \Delta p_{tube} \tag{10}$$

where A is the inner cross-sectional area of the pipe and a is the local sound velocity. Thus, the measurement of the pressure waveform inside the tube is strictly sufficient, since it is possible to assess the direct proportionality between the injected fuel rate and the pressure waveform.

The back pressure for the determination of the injection rate was kept constant and equal to 4 MPa. It was chosen in order to have a significant value comparable with the one inside the combustion chamber during the actual start of the injection process. Moreover, if the back pressure were excessively low, cavitation may occur because of a high velocity fuel injection and considerable variations in the injection rate waveform could occur. An inconvenience of such a measurement

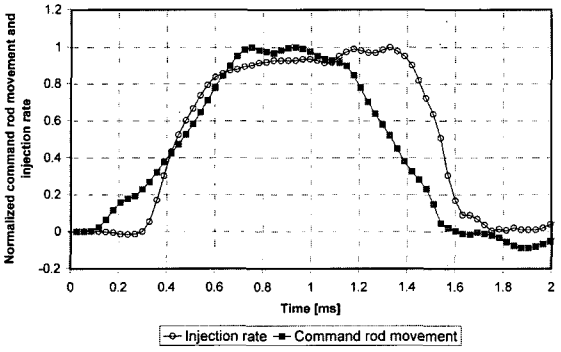

Figure 8. Normalized command rod movement and injection rate (p_{rail} = 120 MPa, ET = 0.9 ms).

method, if compared to others (Takamura *et al.*, 1992), consists of the injection rate waveform which, at the end of the injection, does not immediately return to the base level as it was before the start of injection.

3.2. Command Rod Movement

As regards the needle lift, measured together with the injected fuel rate, here it is worth underlining that the real measurement regards the command rod movement and not strictly the needle lift. This measure considers the elastic release of the command rod-needle assembly. Thus, the command rod drives the needle movement but with a certain delay, reflecting upon the actual start of the injection process.

Moreover, the pressure transducer in the measuring device was located distant from the nozzle position, so a delay was observed between the two recorded signals as Figure 8 shows. This delay consists of the ratio between such a distance and the fuel sound velocity.

In order to determine the injection starting timing, two reference voltages VS_1 and VS_2, as regards the rising part of the fuel rate, and two reference voltages VF_3 and VF_4 for its falling part are to be set. The injection starting time is determined as follows: P_1 and P_2 are the points where the rising part of the injection rate waveform crosses the reference levels VS_1 and VS_2. The point where the straight line passing through P_1 and P_2 intersects the base line represents the start of injection (SOI). The point concerning the end of injection (EOI) is determined in a similar way, i.e. it is the point where the straight line passing through P_3 and P_4, the points where the falling part of the injection rate waveform crosses VF_3 and VF_4, intersects the base line. The fuel injection period t_{inj}, is obtained from the above mentioned starting and ending points (Figure 9).

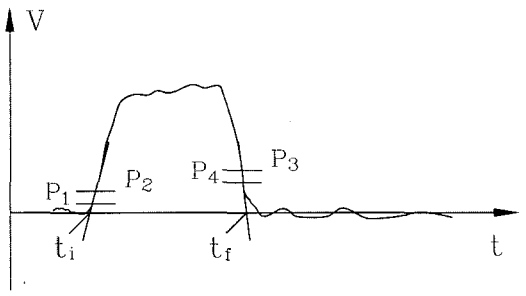

Figure 9. Method to define the duration of injection with respect to its start (t_i) and end (t_f).

3.3. Investigated Control Valves

In the current study, all the investigated injectors were equipped with the same nozzle but different control valves. These valves differ since the discharge properties through the Z hole were progressively varied. Starting from a standard valve, its Z hole was hydro ground in order to achieve the desired increase in its discharge properties. Later, the valve was tested on a hydraulic test bench and the steady state discharge properties were measured for a fixed pressure drop equal to 10 MPa and a back pressure fixed to 6 MPa. As a matter of fact, when injector works, the control volume does not fully deplete, presenting always a back pressure to the inlet fuel flow.

In the following, the injectors equipped with control valves whose Z hole discharge properties were increased are characterized by an increasing numeration. Such a number refers to the proportional increase of flow rate through the Z hole with respect to the standard valve. Thus, the standard injector is identified as '00', '09' refers to the injector whose control valve presents Z hole discharge properties increased up to 9%, etc.

4. INJECTION BEHAVIOUR RESULTS

Three values of rail pressure were considered with reference to medium low, medium high and high injection pressures, equal respectively to 40, 80 and 135 MPa. Figure 10 shows comparisons between experimental and

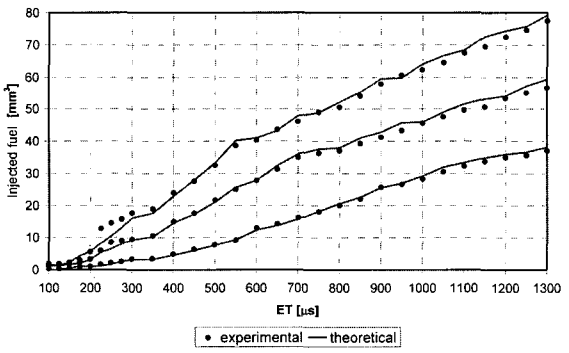

Figure 10. Cumulated fuel injected by the standard injector for three different rail pressures.

theoretical injected fuel. With the exception of an interval where ETs are relatively short, the model seems to be sufficiently reliable.

However, Figure 10 shows only one result of the model, since it was prevalently used in simulating and studying the injection rate.

Preliminary comparisons between theoretical and measured injection rates are shown in Carlucci *et al.* (2003) as regards the standard injector and the '09' modified one. Here, all the rates are shown with respect to only one ET fixed equal to 0.6 ms for the sake of simplicity. Figures 11 to 13 show experimental and theoretical injection rates together with command rod movements as regards the standard injector.

Now, paying attention to the injection process, Figures 14 to 16 show comparisons between experimental and theoretical injection rates with reference to the '09' modified injector. As regards the expected modulation of the first stage of the injection rate, it is difficult to appreciate, but it is always accomplished with an early closure of the needle, due to a quicker velocity. Of course, both experiments and simulation show that the modified injector injects less fuel than the standard one. Thus, in order to inject the same amount of fuel, the '09' modified injector should be excited for a longer time with respect to the standard one. Comparisons with the same ET are useful to verify the theoretical considerations advanced in Amoia *et al.* (1997), where an enlargement of the Z hole was found to lead to such results.

According to the results reported in Figures 11 to 16, an appreciable capability of the model in simulating the injection behaviour may be observed and a good agreement between theoretical and experimental injec-

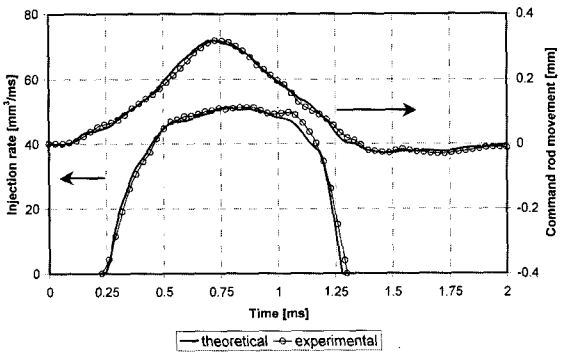

Figure 11. Command rod movement and injection rates for the standard injector (p_{rail} = 135 MPa, ET = 0.6 ms).

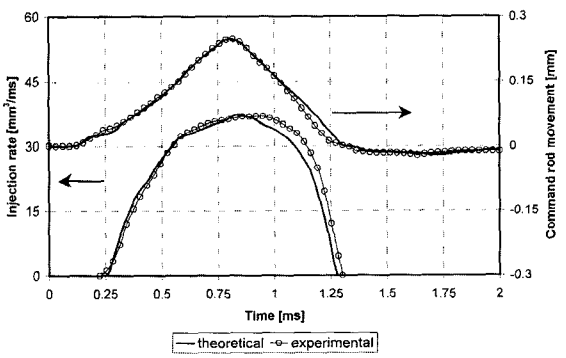

Figure 12. Command rod movement and injection rates for the standard injector (p_{rail} = 80 MPa, ET = 0.6 ms).

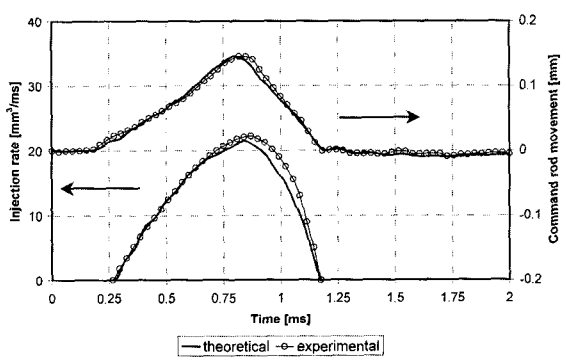

Figure 13. Command rod movement and injection rates for the standard injector (p_{rail} = 40 MPa, ET = 0.6 ms).

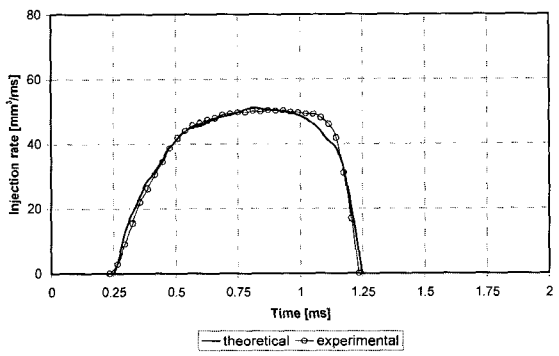

Figure 14. Injection rates for the '09' modified injector (p_{rail} = 135 MPa, ET = 0.6 ms).

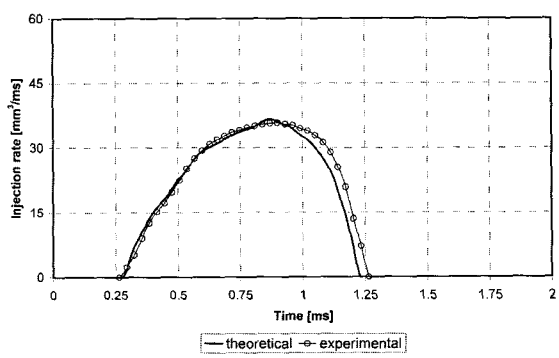

Figure 15. Injection rates for the '09' modified injector (p_{rail} = 80 MPa, ET = 0.6 ms).

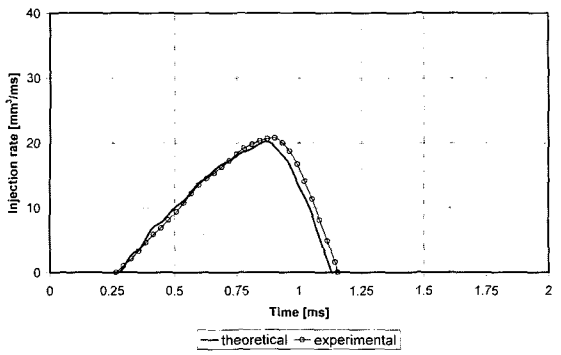

Figure 16. Injection rates for the '09' modified injector (p_{rail} = 40 MPa, ET = 0.6 ms).

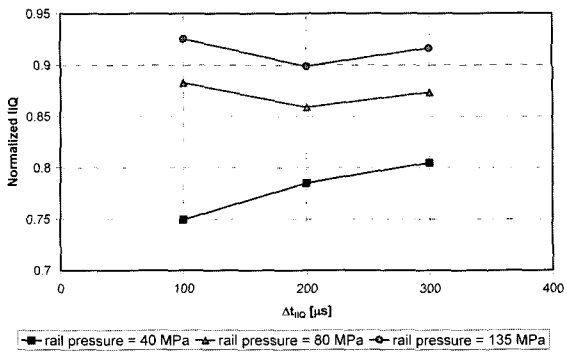

Figure 19. IIQs of the '09' modified injector normalized with respect to the standard one.

tion rates is achieved. As a matter of fact, even if geometrical modifications in the control valve are realized, the model correctly simulates the fuel rates of the modified injector.

As regards the aim of this work, consisting of a modulation of the first stage of injection, injection rates should be superimposed in order to appreciate what happens when '09' modified injectors are used instead of standard ones. However, the slope of the first stage of the injection rate is not clearly defined.

Here, in order to quantify possible variations because of modifications in the control valves, the amounts of cumulated injected fuel, namely initial injection quantity (IIQ), during a fixed time interval, are compared with reference to the two different injectors. Of course, this time interval (Δt_{IIQ}) cannot be fixed once at all (Figure 17).

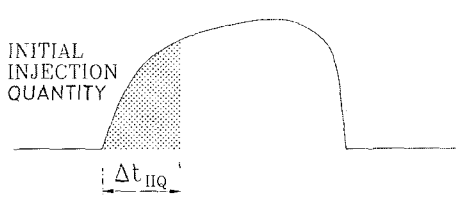

Figure 17. Quantification of the initial injection quantity (IIQ).

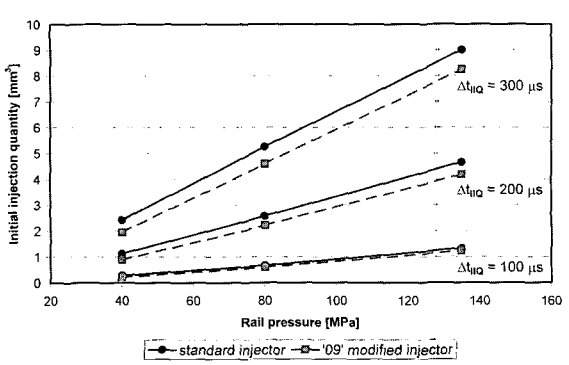

Figure 18. Initial injection quantity vs. rail pressure.

Thus, three time intervals for evaluating IIQ were fixed and comparisons between the IIQs are shown in Figure 18. The reductions in IIQ achieved from the SOI with respect to the standard injection are quantified and shown in Figure 19.

Looking at these results, different trends may be noticed with reference to the three rail pressures. Such a result should be due to the slope of the initial stage of the injection rate which is not constant, as previously mentioned. Anyway, the possibility of modulating the first stage of the injection rate appears evident for medium low rail pressures since a reduction in IIQ amounting to 20÷25% may be achieved.

Nevertheless, it is to be considered that in the last years DI diesel engines have been equipped with high pressure fuel injection systems and maximum injection pressure is going to increase (Mahr, 2002). Then, the current level of modulation of the injection rate, less appreciable for higher injection pressures, could lose its expected capability in controlling the first stage of the combustion process.

In order to achieve more significant variations in the first stage of the injection rate, the model was used to investigate the effects of further increases in the discharge properties of the Z hole. As previously mentioned, the modified valve comes from a standard one whose Z hole has been hydro ground. The effect of such a process, consisting in rounding the inlet of the hole, should be interpreted as a variation of its discharge coefficient which cannot be increased beyond a limit value. Considering such a limit, the model was used in order to predict the effects of further increases in Z hole discharge properties with reference to the IIQ. It is also to be taken into account that an excessive level of hydro grinding in the Z hole may prevent the control volume from depleting, defining limits for minimum injection pressures. The trends previously shown in Figures 18 and

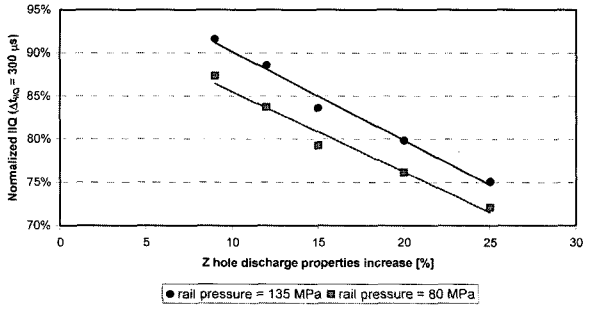

Figure 20. IIQ variations depending on Z hole discharge properties.

19 are found again in Figure 20 where, fixing Δt_{IIQ} equal to 300 μs, further reductions in IIQ are achieved if the discharge properties of the Z hole are increased.

The results shown in Figure 20 present a clearly decreasing trend for both the two pressure levels (80 and 135 MPa). Moreover, a considerable linearity among the results seems to be manifest: the absolute value of the correlation coefficient is equal to 0.993 and 0.986 for 135 MPa and 80 MPa respectively.

Considering the results advanced by the theoretical model, it is possible to extend the trend beyond the limit here fixed for the increase of the Z hole discharge properties. However, such an event would lead to the realization of a particular control valve since simple hydro grinding is no more sufficient. As a matter of fact, it was very difficult to increase the Z hole discharge properties by means of only hydro grinding at an extent greater than 20%.

Finally, according to the suggestions provided during the current research, a series of four control valves whose Z hole discharge properties are increased up to 20% were realized and a new experimental campaign was carried out. Figures 21 and 22 show the results concerning injection rates and command rod movements as regards

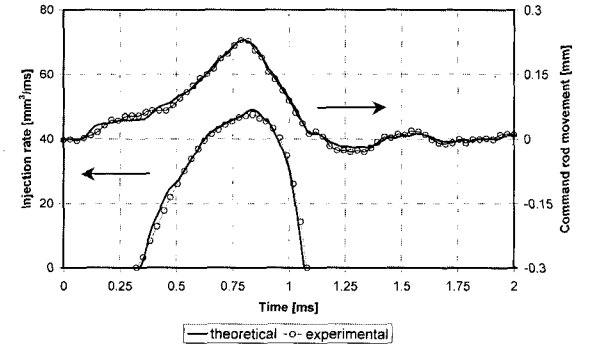

Figure 21. Command rod movement and injection rates for the '20' modified injector (p_{rail} = 135 MPa, ET = 0.6 ms).

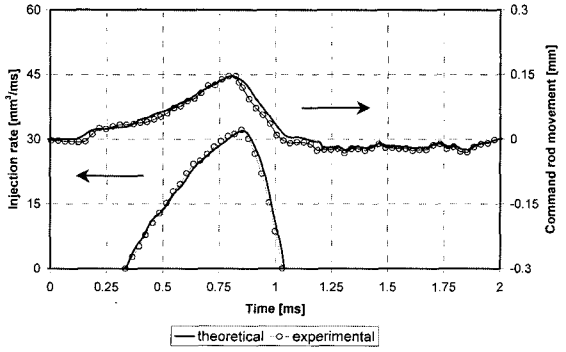

Figure 22. Command rod movement and injection rates for the '20' modified injector (p_{rail} = 80 MPa, ET = 0.6 ms).

two injection rail pressures equal to 135 and 80 MPa respectively. The ET of the solenoid is always fixed to 0.6 ms.

These last comparisons show again the great capability of the model in correctly predicting the injection behaviour for medium-high and high pressure levels of the fuel inside the rail, even if modifications are realized in the piloting stage of the injector. These results verify the proposals advanced with this study.

5. CONCLUSION

The injection behaviour of a CR injector was characterized by simulation and experiments. The model developed for the study of the injection process shows a good reliability, especially in predicting the shape of the injection rate. Thus, a theoretical study concerning the injection behaviour with respect to geometrical and hydraulic modifications is possible.

The current stage of this research activity was focused on simple expedients to modulate and to achieve injection rates different from the standard ones. Both experiments and simulations show that properly modulating injection rate is difficult. However, achieving a definite reduction in the quantity of fuel injected during the first stage of injection is possible.

This first work, only oriented to investigations on the fluid dynamic behaviour of the injector, will be followed by experimental tests to evaluate advantages and disadvantages of modulated injections during the actual engine running. Some preliminary results of the new researches are reported by Carlucci *et al.* (2004).

ACKNOWLEDGEMENT–The authors would like to thank Eng A. Arvizzigno (Bosch-CSIT, Bari, Italy) for the experimental support. A. Giuffrida gratefully thanks professor D. Laforgia for having welcomed him during his training period at the Faculty of Engineering in Lecce and Imagine for the use of the simulation software.

REFERENCES

Amoia, V., Ficarella, A., Laforgia, D., De Matthaeis, S. and Genco, C. (1997). A theoretical code to simulate the behavior of an electro-injector for diesel engines and parametric analysis. *SAE Paper No.* 970349.

Bosch, W. (1996). The fuel rate indicator: A new measuring instrument for display of the characteristics of individual injection. *SAE Paper No.* 660749.

Carlucci, P., Ficarella, A., Giuffrida, A. and Lanzafame, R. (2003). Investigation on realizing fuel rate shaping using a common rail injector. *ASME ICES 2003 Spring Technical Conference*, Salzburg, Austria, May 11–14, 2003.

Carlucci, P., Ficarella, A., Chiara, F., Giuffrida, A. and Lanzafame, R. (2004). Preliminary studies on the effects of injection rate modulation on the combustion noise of a common rail diesel engine. *SAE Paper No.* 2004-01-1848.

De Risi, A., Donateo, T. and Laforgia, D. (2002). An application of multi-criteria genetic algorithms to the optimization of a common rail injector. *2002 ASME ICE Spring Technical Conference*, Rockford, USA, April 14–17.

Desantes, J. M., Arregle, J. and Rodriguez, P. J. (1999). Computational model for simulation of diesel injection systems. *SAE Paper No.* 1999-01-0915.

Digesù, P., Ficarella, A., Laforgia, D., Bruni, G. and Ricco, M. (1994). Diesel electro injector: A numerical simulation code. *SAE Paper No.* 940193.

Erlach, H., Chmela, F., Cartellieri, W. and Herzog, P. (1995). Pressure modulated injection and its effect on combustion and emissions of a HD diesel engine. *SAE Paper No.* 952059.

Ficarella, A., Laforgia, D. and Landriscina, V. (1999). Evaluation of instability phenomena in a common rail injection system for high speed diesel engines. *SAE Paper No.* 1999-01-0192.

Henein, N. A., Lai, M. C., Singh, I. P., Zhong, L. and Han, J. (2002). Characteristics of a common rail diesel injection system under pilot and post injection modes. *SAE Paper No.* 2002-01-0218.

Herzog, P. (1989). The Ideal Rate of Injection for Swirl Supported Diesel Engines, IMechE Seminar "Diesel Fuel Injection Systems", Birmingham, UK, October 10–11.

Kampmann, S., Dittus, B., Mattes, P. and Kirner, M. (1996). The influence of hydro grinding at VCO nozzles on the mixture preparation in a DI diesel engine. *SAE Paper No.* 960867.

Klomp, E. D. (1999). Valve-Covered-Orifice (VCO) fuel injection nozzle delivery analysis. *Atomization and Sprays*, **9**, 541–579.

Imagine (2000). AMESim® Standard Fluid Properties. Technical Bulletin **117**. Roanne. France.

Imagine (2002). AMESim® Version 4.0. March Roanne. France.

Lee, J. H., Cho, S., Lee, S. Y. and Bae, C. (2002). Bouncing of the diesel injector needle at the closing stage. *Proc. Institution of Mechanical Engineers*, **216**, *Part D: J. Automobile Engineering*, 691–700.

Mahr, B. (2002). Future and potential of diesel injection systems. *Proc. THIESEL 2002 Conference on Thermo- and Fluid-Dynamic Processes in Diesel Engines*, Valencia, Spain, September 10–13.

Nehmer, D. A. and Reitz, R. D. (1994). Measurements of the effects of injection rate and split injections on diesel engine soot and NOx emissions. *SAE Paper No.* 940668.

Nurick, W. H. (1976). Orifice cavitation and its effect on spray mixing. *ASME J. Fluids Engineering*, **98**, 681–687.

Schmidt, D. P. and Corradini, M. L. (1997). Analytic prediction of the exit flow of cavitating orifices. *Atomization and Sprays*, 7, 603–616.

Stumpp, G. and Ricco, M. (1996). Common rail-an attractive fuel injection system for passenger car DI diesel engines. *SAE Paper No.* 960870.

Takamura, A., Ohta, T., Fukushima, S. and Kamimoto, T. (1992). A study on precise measurement of diesel fuel injection rate. *SAE Paper No.* 920630.